CHEMISTRY OF MATERIALS

ARTICLE

pubs.acs.org/cm

Investigating the Role of Zeolite Nanocrystal Seeds in the Synthesis of Mesoporous Catalysts with Zeolite Wall Structure

Xiaobin Wang,[†] Xiongfu Zhang,[*,†] Yao Wang,[†] Haiou Liu,[†] Jieshan Qiu,[*,†] Jinqu Wang,[†] Wei Han,[‡] and King Lun Yeung[*,‡]

[†]State Key Laboratory of Fine Chemicals, School of Chemical Engineering, Dalian University of Technology, Dalian 116024, P.R. China

[‡]Department of Chemical and Biomolecular Engineering, The Hong Kong University of Science and Technology, Clear Water Bay, Kowloon, Hong Kong, P.R. China

ABSTRACT: Mesoporous titania-silica catalysts were prepared by hydrothermal conversion from synthesis solutions containing a zeolite structure directing agent (TPA^+) and a porogen (CTA^+). Syntheses were carried out with and without addition of zeolite seeds (i.e., TS-1 and Sil-1 nanocrystals). Catalysts prepared in the presence of zeolite nanocrystal seeds have greater proportions of tetrahedrally coordinated titanium, which correlate well with the detection of zeolite SBU fragments and ring-structure by TOF-SIMS and FTIR. The incorporation of titano-silicates and zeolite structural units in the mesopore walls could explain the better activity and stability of these catalysts (Ti-MT1 and Ti-MS1) compared to the catalyst prepared by the conventional method (Ti-MCM-41). The similarity in the reactivity of catalysts prepared from TS-1 and Sil-1 nanocrystal seeds dispels the idea that the seeds are merely a source of the zeolite fragments incorporated in the pore walls but instead suggests that the seeds play an active role to stabilize and promote the incorporation of SBU from the solution.

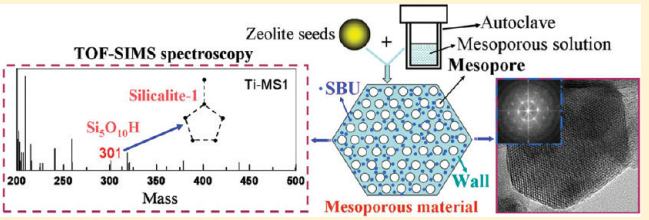

KEYWORDS: titania-silica, TS-1, MCM-41, hydroxylation reaction, catalyst deactivation

1. INTRODUCTION

Titanium-containing catalysts find applications in fine chemical synthesis,[1−4] pollution abatement,[5−10] and solar energy conversion.[11,12] Microporous titanium silicates catalyze important selective oxidation,[13,14] hydroxylation,[15−19] and ammoxidation reactions.[20] However, the narrow pore size of the zeolite limits the reactions to small molecules. The discovery of mesoporous materials (i.e., M41S, SBA, MSU) in early 1990[21−24] spurred innovations in catalyst preparation and exploration of their applications in chemical synthesis,[24−26] environment,[27−32] and even in electronics and biomedicine.[33,34]

A considerable effort was invested in developing mesoporous titania and titania-silica catalysts since the early works of Corma et al.[35] and Tanev et al.[36] The goal is to develop more active catalysts that are stable under severe reaction conditions.[37,38] Various approaches including preparing mesoporous catalysts with thick pore walls[39] and incorporating zeolitic structures[40−46] had been reported. Mesoporous catalysts with excellent activity and good hydrothermal stability had been synthesized from mixtures containing zeolite nanoparticles.[47−56] It is believed that the zeolite nanocrystals either dissolved during the synthesis into zeolitic fragments that are then incorporated into the pore wall or actively nucleate primary and secondary zeolite building units that are inserted into the wall structure. This work attempts to clarify the role of the zeolite seeds in the synthesis of the mesoporous titania-silica catalysts.

Three mesoporous catalysts were prepared from identical synthesis solutions and conditions. Ti-MCM-41 was prepared without addition of zeolite seeds, while Ti-MT1 and Ti-MS1 were prepared from synthesis mixtures containing TPA-TS-1 and TPA-Sil-1 nanocrystal seeds, respectively. We had confirmed in prior studies[17−19,57] that both TPA-TS-1 and TPA-Sil-1 nanocrystals can seed the growth of TS-1 zeolite. Chiang and co-workers also prepared mesoporous silicas and materials of varied morphologies using silicalite nanocrystals.[58−61] If the seeds function merely as source of zeolitic structure, it is expected that mesoporous catalysts prepared from the two seed materials will differ significantly in composition and activity. However, if the seeds promote the formation of primary and secondary zeolite building units, the catalysts will display similar chemistry. The morphology and structure of the catalysts were examined by electron microscopy, X-ray diffraction, and N_2 physisorption. Titanium incorporation was monitored by X-ray fluorescence and X-ray photoelectron spectroscopy methods, and evidence of zeolitic structures were sought by time-of-flight secondary mass spectroscopy and Fourier transform infrared spectroscopy. Diffuse reflectance UV−vis spectroscopy was used to probe the coordination environment of the titanium ion in the catalysts. Benzene, phenol, and styrene hydroxylation were used as probe reactions.

Received: June 8, 2011
Revised: August 29, 2011
Published: October 03, 2011

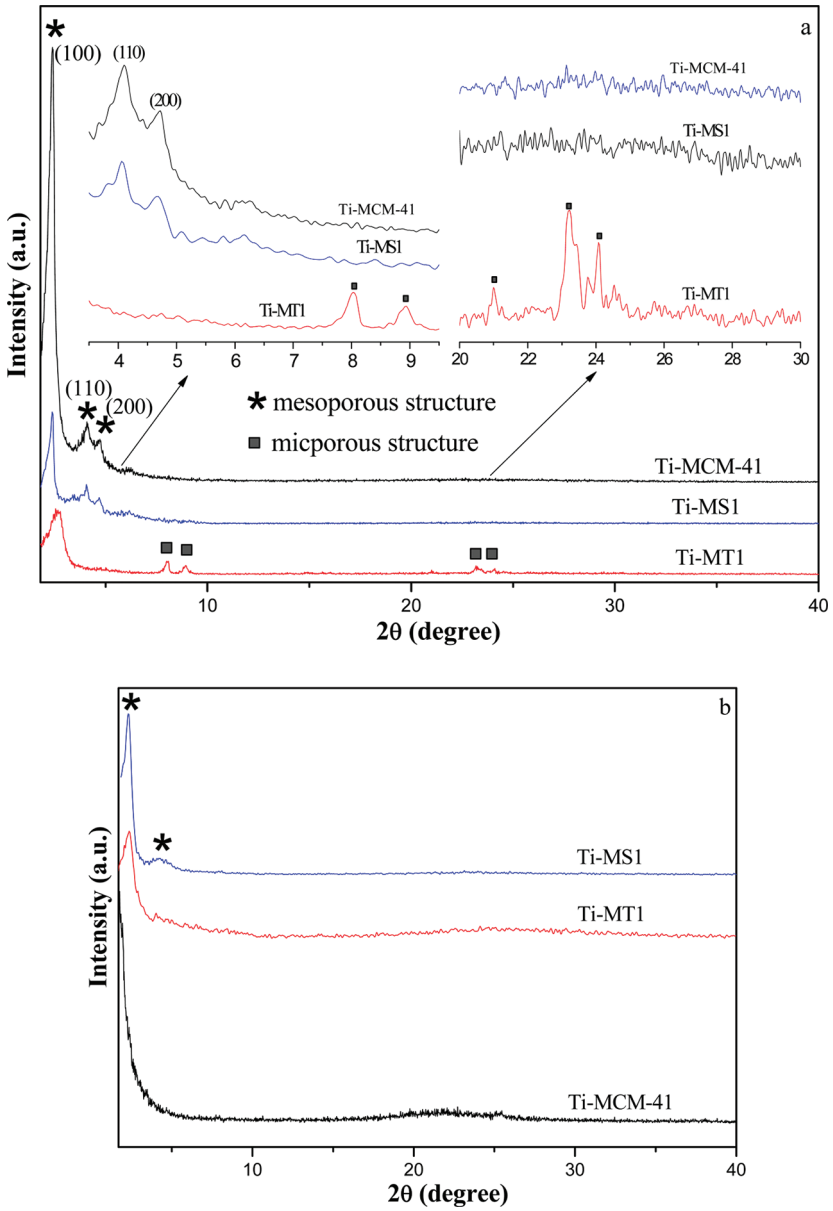

Figure 1. X-ray diffraction patterns of calcined Ti-MCM-41, Ti-MT1, and Ti-MS1 (a) before and (b) after hydrothermal treatment in boiling water for 120 h.

2. EXPERIMENTAL SECTION

2.1. Chemicals and Reagents. The reagents for the synthesis of the zeolite nanocrystal seeds and mesoporous catalysts included tetraethyl orthosilicate (TEOS, 98%, Tianjin Kermel), tetrabutyl orthotitanate (TBOT, 98.5%, Beijing Xingjin), tetrapropylammonium hydroxide (TPAOH, 17 wt %, prepared in the laboratory), and cetyltrimethylammonium bromide (CTABr, Tianjin Kermel). The former was prepared in the laboratory according to the procedure published in our prior works.[17] Benzene (99.5%), phenol (98.5%), styrene (98.0%), and hydrogen peroxide (H_2O_2, 30%) used in the reaction studies were purchased from Tianjin Kermel Chemical Reagent Ltd. Isopropyl alcohol (IPA, 99.7%) and acetone (ACE, 99.5%) solvents were also supplied by Tianjin Kermel.

2.2. Preparation and Characterization of Mesoporous Catalysts. Three titanium containing mesoporous catalysts were prepared, Ti-MCM-41 by a conventional method,[62] and the Ti-MT1 and Ti-MS1 with addition of TS-1 and Sil-1 nanocrystal seeds, respectively. The 200 nm Sil-1 seeds were prepared from 1 SiO_2:0.22 TPA_2O:19.2 H_2O by hydrothermal synthesis at a temperature 398 K for 8 h.[17,63] The seeds were recovered by a series of centrifugation and washing steps to remove the coarse particles and unreacted gels and to adjust the final pH to 7. The TS-1 seeds (ca. 200 nm) were prepared by a similar procedure from a synthesis solution containing 1 SiO_2:0.02 TiO_2:0.22 TPA_2O:19.2 H_2O.[17] The seed stocks were then diluted to 2 wt % colloidal seed suspensions.

The preparation of the mesoporous catalysts starts by slowly adding 2.1 mL of TEOS to 3.5 mL of TPAOH solution under vigorous mixing, followed by the dropwise addition of 0.06 g of TBOT dissolved in dry isopropanol.[64,65] The resulting solution was heated to ca. 360 K for 40 min to remove the alcohols. Water was added to make up for the lost volume, and the final solution was aged for 24 h at room temperature.

dx.doi.org/10.1021/cm201619y |*Chem. Mater.* 2011, 23, 4469–4479

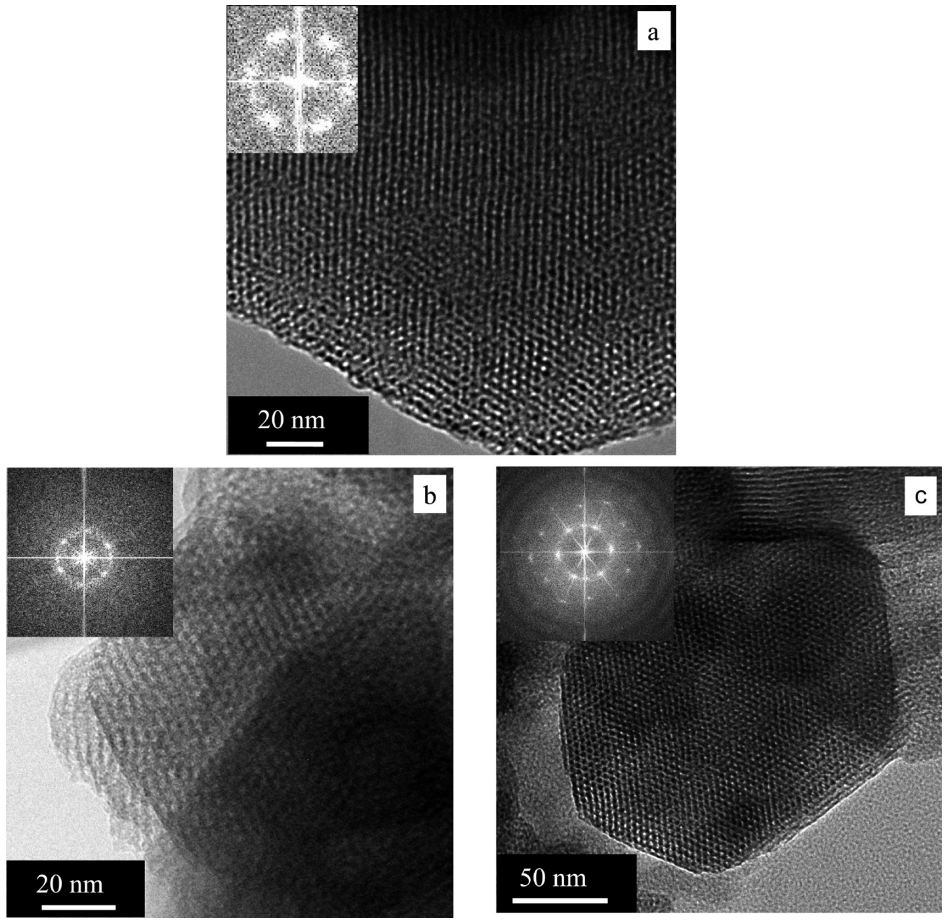

Figure 2. Transmission electron microscope images and electron diffraction patterns of (a) Ti-MCM-41, (b) Ti-MT1, and (c) Ti-MS1.

This solution was slowly added to a CTABr solution prepared by dissolving 1.5 g of CTABr in 20 mL of deionized distilled water under constant mixing to give a synthesis mixture with a molar composition of 1 SiO_2:0.02 TiO_2:0.18 TPA_2O:0.4 CTABr:250 H_2O. The seeds (ca. 0.01 to 0.05 wt %) were added to the synthesis solution, and the mixture was stirred for 2 h at ca. 308 K, before transferring the mixture in an autoclave for synthesis in an oven at 373 K for 24 h. Ti-MCM-41 was prepared from the same synthesis solution but without the zeolite seeds and the synthesis lasted 48 h. The mesoporous catalysts were recovered by filtration and washed with distilled water until a neutral pH was reached. The catalysts were dried overnight before calcining in air at 823 K for 6 h after heating at 1 K•min^{-1}. Mesoporous MCM-41 silica was also prepared for comparison.

The mesoporous catalysts were characterized by D/Max 2400 Rigaku X-ray diffractometer (XRD) with a Cu−Kα radiation (λ = 0.1542 nm) at a voltage of 40 kV and 50 mA, and the nitrogen sorption isotherms were measured by Coulter SA3100 surface area and pore size analyzer after outgassing for 2 h at 403 K. The pore size was determined from the X-ray diffraction and N_2 physisorption data according to the equation derived by Kruk et al.[66] for ordered mesoporous solids. The mesopore size and micropore size distributions were calculated using the Barret-Joyner-Halenda (BJH) method and the Horvath−Kawazoe (HK) model. The catalysts were also examined by a JEOL JEM 2010 transmission electron microscope operated at an accelerating voltage of 200 kV and beam current of 100 pA.

The catalyst composition and chemistry were analyzed by X-ray fluorescence spectroscopy (XRF), X-ray photoelectron spectroscopy (XPS), time-of-flight secondary ion mass spectroscopy (TOF-SIMS), Fourier transform infrared spectroscopy (FTIR), and diffuse reflectance UV−vis spectroscopy. The bulk elemental composition of the catalysts were determined by a JEOL JSX-3201Z X-ray fluorescence spectrometer and confirmed by energy dispersive X-ray spectroscopy (EDXS, Oxford Instruments) during TEM imaging. The surface elemental composition was obtained by an XPS (Physical Electronics PHI 5000) using a monochromatic Al X-ray source (1486.6 eV). Both regular and high-resolution scans were gathered, and the data were plotted with respect to the binding energy. The samples were analyzed by an ION-TOF GmbH TOF-SIMS V spectrometer equipped with 25 keV Bi^{3+} cluster ion source that has an average pulsed current of 0.1 pA. Spectra were obtained and averaged over three 200 × 200 μm^2 areas. Each spectrum was collected for 40 s at ion flux dosage of less than 2 × 10^{11} ions/cm^2. The infrared and UV−vis spectra of the catalysts were respectively obtained by a Bruker EQUINOX55 FTIR after pressing into a wafer with KBr diluent and by a JASCO V-550 UV−vis spectrometer with diffuse reflectance accessories using $BaSO_4$ as an internal standard.

2.3. Benzene, Phenol, and Styrene Hydroxylation Reactions. The three titanium-containing mesoporous catalysts (i.e., Ti-MCM-41, Ti-MT1, Ti-MS1), TS-1, and MCM-41 were investigated for the hydroxylation of benzene, phenol, and styrene in a batch reactor. The temperature of the reactor was maintained by a water jacket at the reaction temperature of 358 K. A typical reaction mixture contains 0.1 g of catalyst, 10 g of aromatic reactant, 23 mL of dry acetone, and 4.2 mL of H_2O_2, and each reaction lasted for six hours. Samples were drawn every 60 min, filtered, and analyzed by a gas chromatograph (GC7890F, Shanghai Techcomp Limited) equipped with a flame ionization detector and a capillary column (SE-30, l 50 m × Φ 0.32 mm ×0.5 μm).

dx.doi.org/10.1021/cm201619y |*Chem. Mater.* 2011, 23, 4469–4479

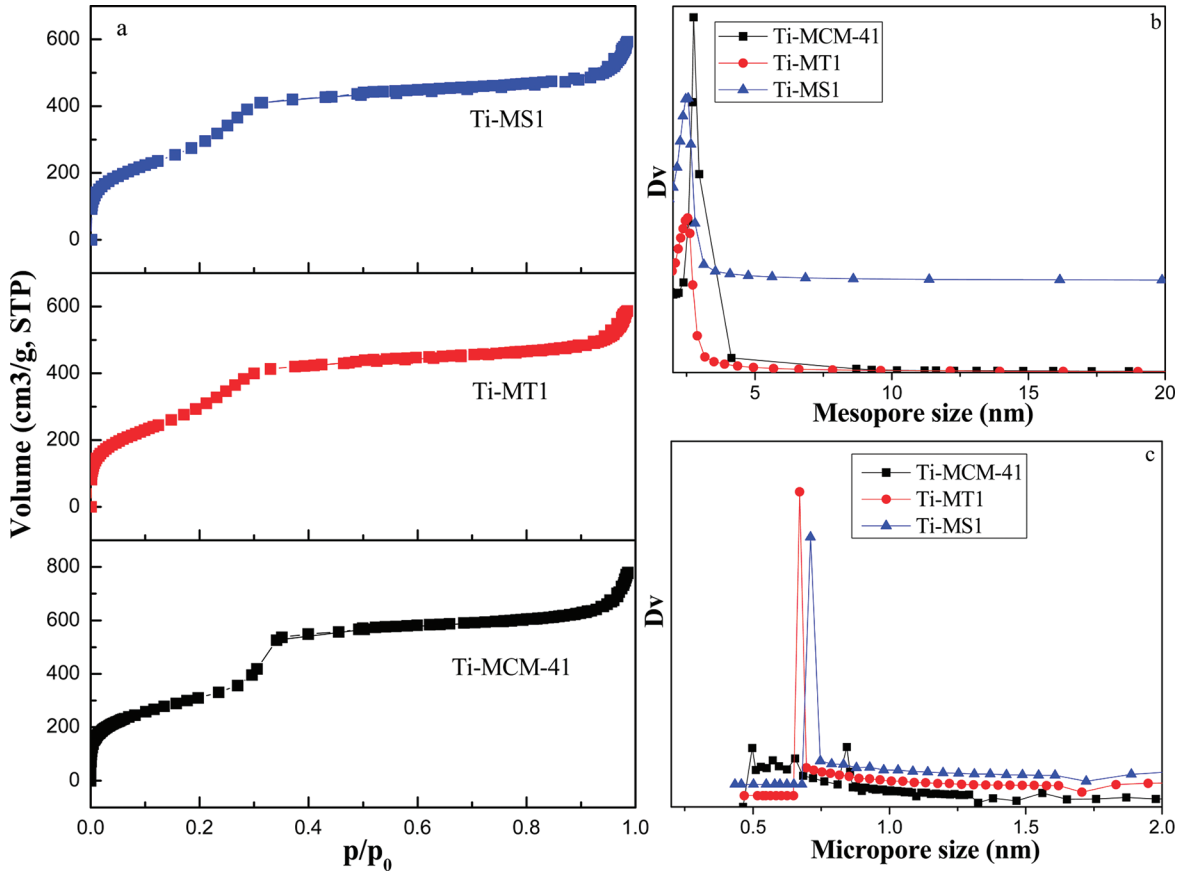

Figure 3. (a) Nitrogen adsorption/desorption isotherms, (b) mesopore size distribution, and (c) micropore distribution of Ti-MCM-41, Ti-MT1, and Ti-MS1.

Catalyst deactivation and regeneration were investigated by reusing the catalysts three successive times in the reactions. The reactant conversion and product selectivity were monitored in the study. For the deactivation study, the spent catalysts were filtered, washed, and dried between reactions, while for the regeneration study the catalysts were also calcined in air at 823 K for 5 h.

3. RESULTS AND DISCUSSION

3.1. Structure and Physical Properties of the Mesoporous Catalysts. Ti-MCM-41, Ti-MT1, and Ti-MS1 prepared by conventional methods and with addition of TS-1 and Sil-1 nanocrystal seeds were characterized by X-ray diffraction. The powder X-ray diffraction pattern of Ti-MCM-41 in Figure 1a displays the (100), (110), (200), and (210) Bragg peaks that are characteristic of mesoporous materials with a high degree of hexagonal symmetry.[21] The diffractogram of Ti-MS1 indicates that a similar high degree of hexagonal pore symmetry was maintained with the addition of Sil-1 seeds in the synthesis. On the other hand, Ti-MT1 prepared from TS-1 seeds displays a weak (100) peak, and the (110), (200), and (210) Bragg peaks are missing indicating poor pore symmetry and greater disorder. Also unlike Ti-MCM-41 and Ti-MS1, Ti-MT1 displays weak (011), (020), (051), (−303), and (−313) diffaction peaks belonging to the original TS-1 nanocrystal seeds. This suggests TS-1 was somehow incorporated, and a composite structure consisting of distinct meso- and microporous phases exists in Ti-MT1. The experimental findings indicate that Sil-1 seeds were more suitable for preparing single phase mesoporous catalyst, and TS-1 seeds being more stable led to a composite of mesoporous titania-silica and TS-1 zeolite.

The high resolution transmission electron micrographs of the mesoporous catalysts are shown in Figure 2 along with their corresponding electron diffraction patterns. The hexagonal pore symmetry of Ti-MCM-41 and Ti-MS1 samples are clearly seen from their micrographs in Figures 2a and 2c, respectively. Also, their electron diffraction patterns are consistent with the *p6* symmetry and suggest a long-range order. Measurements showed that Ti-MCM-41 and Ti-MS1 have comparable pore size of ca. 2.5 nm. The d (100) spacing of Ti-MS1 is 3.5 nm, which is similar to the X-ray diffraction result. Ti-MT1 has more defects in its pore structure (i.e., Figure 2b), which is possibly the result of embedded zeolite domains and nanocrystals. This result is consistent with the appearance of TS-1 diffraction peaks in its X-ray diffraction pattern.

The N_2 physisorption isotherms of the mesoporous catalysts are plotted in Figure 3a, and the specific BET surface area, pore size, and specific pore volume are listed in Table 1. All three catalysts have a type IV isotherm and display a step increase at relative pressures between 0.2 and 0.4 from capillary condensation in the mesopores. The increase of adsorption volume at the higher relative pressure of 0.9−1.0 indicates that the samples contain large meso- and macropores from interparticle spaces. The mesopore size distribution was calculated by the BJH method and plotted in Figure 3b. Figure 3b shows Ti-MCM-41, Ti-MT1, and Ti-MS1 are

dx.doi.org/10.1021/cm201619y |*Chem. Mater.* 2011, 23, 4469–4479

Table 1. Properties of Ti-MCM-41, Ti-MT1, and Ti-MS1 Catalysts

catalysts	d_{100}[a] (nm)	a_0 (nm)	pore size[b] (nm)	wall thickness[c] (nm)	BET surface area (m^2/g)	pore volume[d] (cm^3/g)	micropore volume (cm^3/g)[e]	SiO_2/TiO_2 molar ratio from XPS	SiO_2/TiO_2 molar ratio from XRF	SiO_2/TiO_2 molar ratio from EDXS
Ti-MCM-41	3.7	4.3	2.7 (3.1)	1.6	1138	1.04		66.6	66.8	76.9
Ti-MT1	3.3	3.8	2.5 (2.7)	1.3	1106	0.88	0.18	65.6	63.1	65.8
Ti-MS1	3.7	4.3	2.6 (3.0)	1.7	1046	0.88	0.11	66.6	62.9	66.4

[a] Calculated from XRD analysis. $a_0 = 2d_{100}/3^{1/2}$. [b] Pore sizes were determined from the adsorption branch of nitrogen isotherm using the BJH model, and the values in parentheses were calculated from the equation derived by Kruk et al.[66] [c] Wall thickness = a_0 - pore size. [d] The pore volume was calculated from the volume adsorbed of P/P_0 at 0.98. [e] Calculated from t-plot analysis.

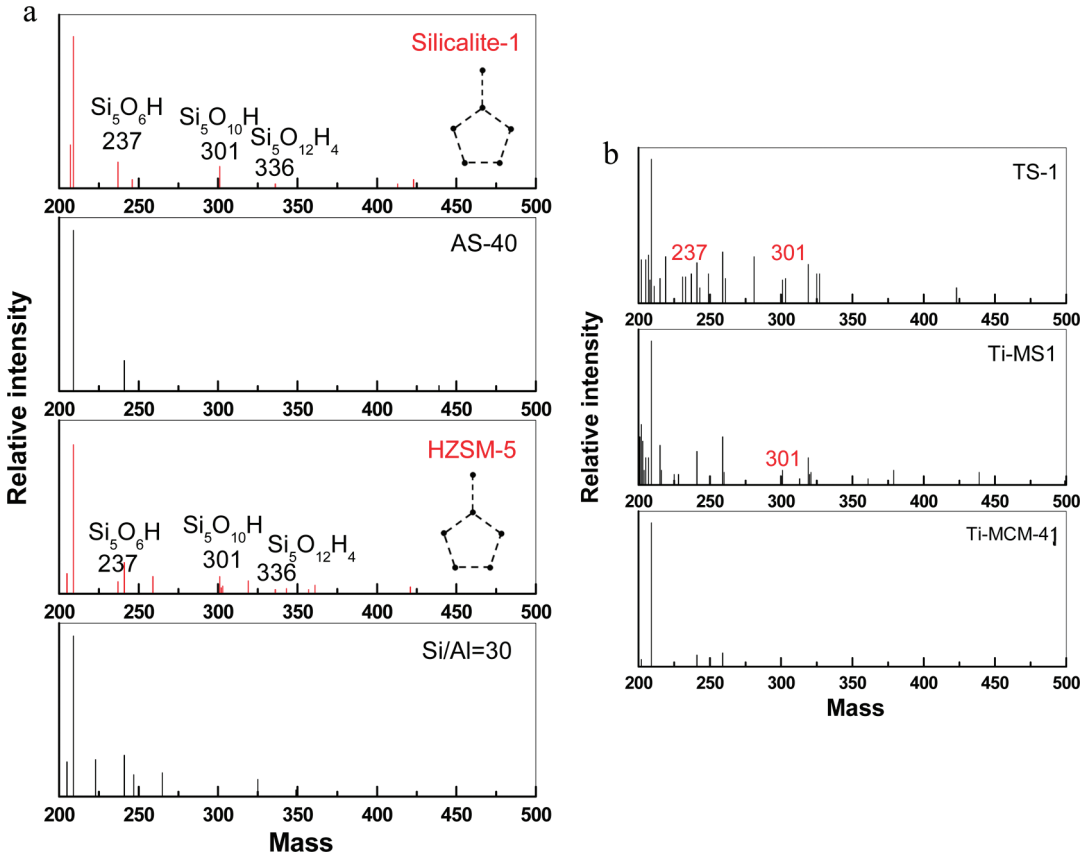

Figure 4. TOF-SIMS spectra of (a) standard samples (inset: SBU of MFI zeolite) and (b) TS-1, Ti-MCM-41, and Ti-MS1.

mesoporous with pore diameters of 2.7 nm, 2.5 nm, and 2.6 nm, respectively. The micropore size distribution calculated by the HK method is included in Figure 3c. Ti-MCM-41 does not have any micropores, while Ti-MT1 and Ti-MS1 prepared from TS-1 and TS-1 nanocrystals have micropores of 0.67 and 0.71 nm, respectively. This suggests the possible presence of a zeolite structure in these materials. The micropore volumes of Ti-MT1 and Ti-MS1 are 0.18 and 0.11 cm^3/g, respectively. Micropores in the Ti-MS1 could be attributed to zeolite structures incorporated in the pore wall.

The hydrothermal stability of the mesoporous catalysts was compared by boiling the catalysts in water for 120 h. Figure 1b shows Ti-MCM-41 prepared by conventional method lost its mesoporous structure after the treatment, which is consistent with prior reports.[14,15] Ti-MS1 and Ti-MT1 were more stable and survived the treatment process. Their diffraction patterns suffered a decrease in overall signal intensity but otherwise displayed the same diffraction peaks as the original catalysts. The Ti-MS1 retained the (100), (110), and (200) Bragg peaks, a good indication that the hexagonal pore symmetry was preserved. After hydrothermal treatment, the XRD peaks associated with TS-1 nanocrystals disappear for Ti-MT1 and could be due to the dissolution of the zeolite during hydrothermal treatment. Similar dissolution of TS-1 was observed and reported by Zhou et al.[67] The improved hydrothermal properties of Ti-MS1 can be attributed to the presence of more zeolitic structures compared to Ti-MCM-41 and a thicker pore wall than Ti-MT1. Indeed, the thickness of the pore wall estimated from the mean diameter of the mesopores obtained by N_2 physisorption and d_{100} spacing from XRD[66] was found to be 1.6 nm for Ti-MCM-41, 1.3 nm for Ti-MT1, and 1.7 nm for Ti-MS1. The partial incorporation of zeolite nanocrystal seeds within the mesoporous material could generate defects and could explain the poorer stability of Ti-MT1.

dx.doi.org/10.1021/cm201619y |*Chem. Mater.* 2011, 23, 4469–4479

Normal X-ray diffraction cannot detect zeolites less than 4−5 unit cells in size, but it is possible using the ToF-SIMS method developed by Yeung et al.[68] ToF-SIMS pulses a beam of ions on the sample, abrading a layer of the surface. The desorbed and ionized fragments are then analyzed by mass spectrometer. It was postulated that secondary building units can survive the fragmentation of the zeolite phase due to their greater stability and could be used to detect presence of zeolite phase in materials. Figure 4a illustrates the technique on MFI zeolite samples. The TOF-SIMS of Sil-1 and TS-1 zeolites showed fragments that correspond 5-Si fragment from the 5−1 secondary building unit of MFI zeolites (i.e., mass values of 237, 301 and 336) that are absent in amorphous silica (Ludox AS-40) and aluminosilicate (Si/Al = 30). The identified SBU fragments are independent of zeolite source (i.e., laboratory or commercial), size (i.e., 70 nm to 10 μm), form (i.e., powder, film, or coating), and composition (i.e., Si/Al = 20 to ∞).[68] The TS-1 zeolite also has the signature mass at 237 and 301 (Figure 4b). These five-membered ring SBU fragments were absent in Ti-MCM-41 catalysts prepared by the conventional method but were detected in Ti-MS1 catalysts (Figure 4b) even though the zeolite structure was not evident from the other techniques (i.e., XRD, TEM, and N_2 physisorption). This result strongly suggests that the incorporation of the zeolitic structure in its thick pore wall is responsible for the excellent hydrothermal stability of Ti-MS1.

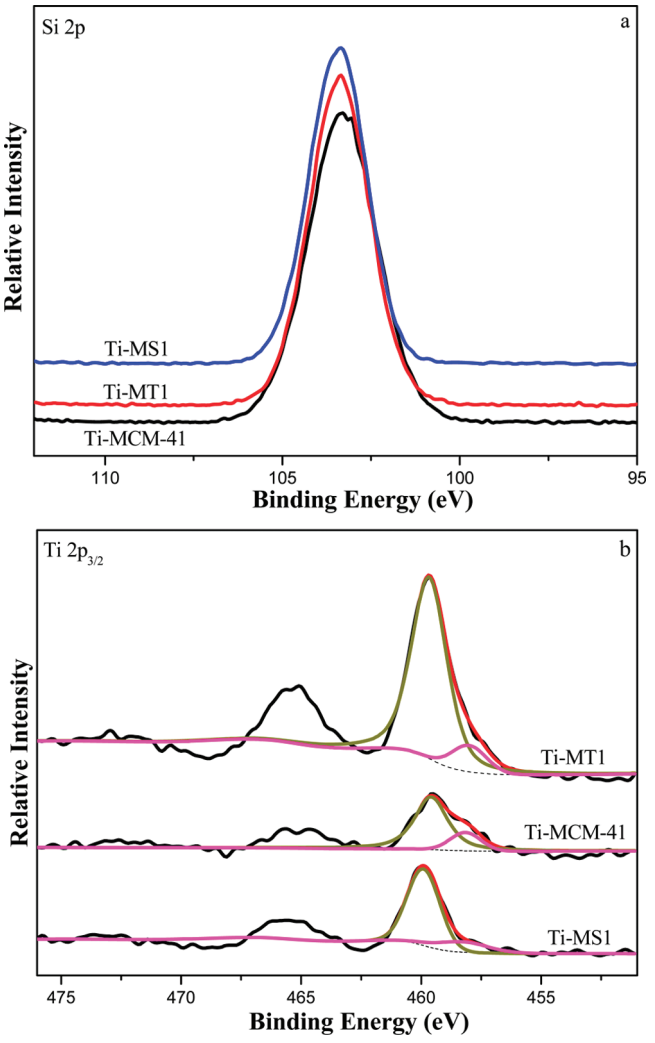

Figure 5. X-ray photoelectron spectra of (a) Si 2p and (b) Ti $2p_{3/2}$ of Ti-MCM-41, Ti-MT1, and Ti-MS1.

3.2. Elemental Composition and Chemistry of the Mesoporous Catalysts. The bulk and surface compositions of the mesoporous catalysts were analyzed by X-ray fluorescence and X-ray photoelectron spectra, and their SiO_2/TiO_2 ratios are listed in Table 1. All three catalysts have comparable bulk and surface compositions. Ti-MCM-41 shows a slight surface enrichment of TiO_2. XPS could provide important information on the chemical state and coordination of titanium ion in the mesoporous catalysts.[69,70]

Figure 5 plots the Si 2p and Ti $2p_{3/2}$ spectra of the catalysts. The Si 2p binding energy of 103 eV was assigned to Si−O−Si and was found in all three catalysts (Figure 5a). The Ti $2p_{3/2}$ binding energies were measured 458.8, 459.3, and 460 eV for Ti-MCM-41, Ti-MT1, and Ti-MS1, respectively. Earlier works on titania-silica mixed oxides[71,72] and titanium silicalites[73,74] identified the photoelectron transition at 460 eV belongs to the titanium in a tetrahedral position of the silicalite lattice, while

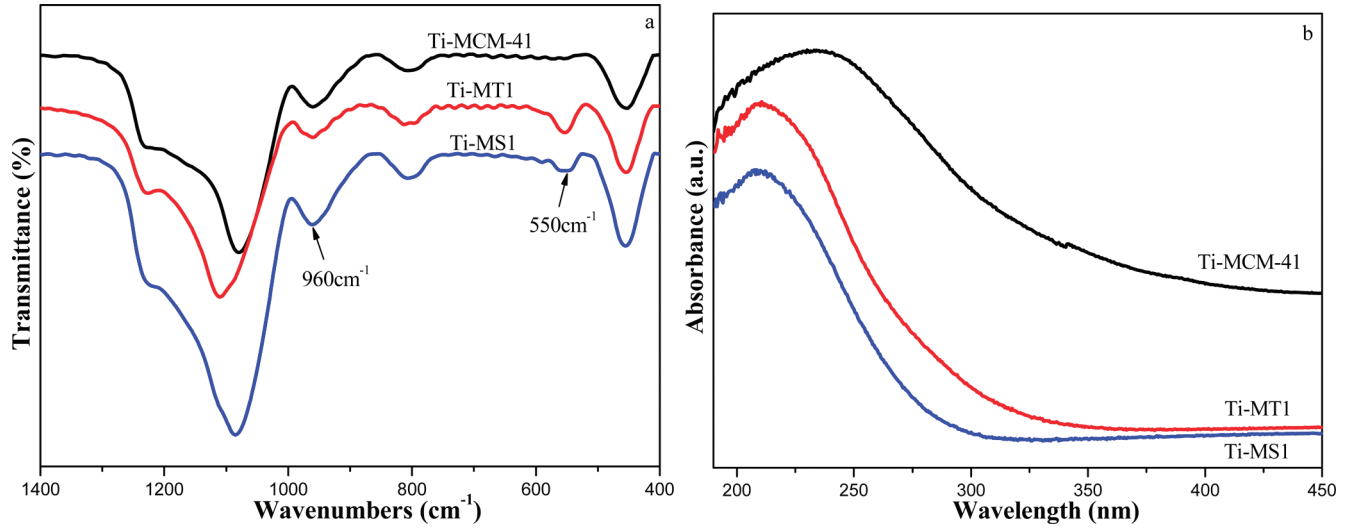

Figure 6. Plots of (a) Fourier transform infrared spectra and (b) diffuse reflectance UV−vis spectra of Ti-MCM-41, Ti-MT1, and Ti-MS1.

dx.doi.org/10.1021/cm201619y |*Chem. Mater.* 2011, 23, 4469–4479

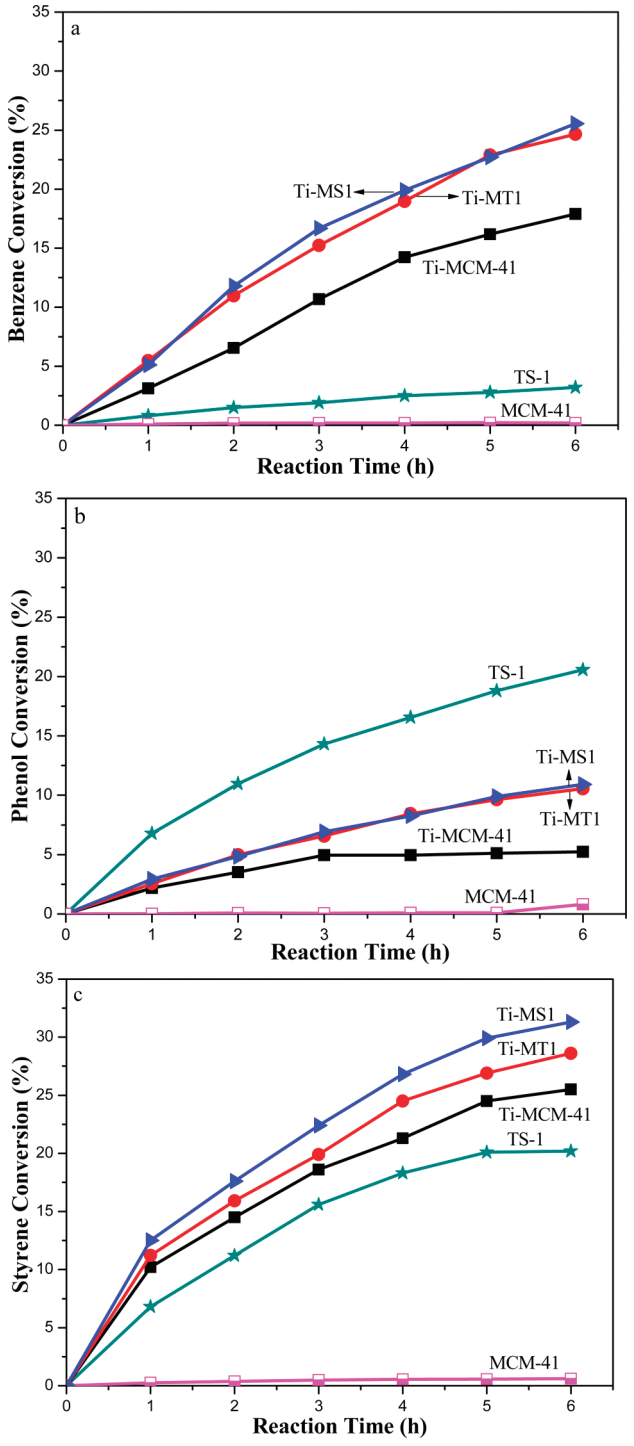

Figure 7. Plots of (a) benzene, (b) phenol, and (c) styrene conversion over Ti-MCM-41, Ti-MT1, and Ti-MS1 mesoporous catalysts and TS-1 and MCM-41.

the transition at 458 eV originates from titanium species with octahedral coordination. The ratios of tetra- to octa-coordinated titanium were estimated from peak deconvolution to be 1.1, 1.5, and 1.5 for Ti-MCM-41, Ti-MT1, and Ti-MS1, respectively. The results indicate that mesoporous catalysts prepared with addition of zeolite seeds possess tetrahedrally coordinated titanium atoms and display zeolite-like character, while most of the titanium found in Ti-MCM-41 is octahedrally coordinated.

Complementary spectroscopic techniques including FTIR and diffuse reflectance UV−vis spectroscopy were done on the catalyst samples. Figure 6a shows that Ti-MT1 and Ti-MS1 have an obvious band at 550 cm^{-1} that is generally assigned to the five-membered ring zeolitic structure. It suggests Ti-MS1 catalyst contains MFI zeolite SBU which is also detected by TOF-SIMS. The band of 550 cm^{-1} is absent in Ti-MCM-41 as to be expected in purely mesoporous materials.[21] It may be tempting to assign the band at 960 cm^{-1} for Ti-MT1 and Ti-MS1 to indicate tetrahedrally coordinated titanium in titania silicalite matrix, but a similar band could also originate from silanol groups found on mesoporous materials (e.g., Ti-MCM-41 and MCM-41). Diffuse reflectance UV−vis spectroscopy can give important information on the coordination of titanium. Figure 6b plots the UV−vis spectra of Ti-MCM-41, Ti-MT1, and Ti-MS1 catalysts. Ti-MCM-41 has a broad absorption band at 230 nm belonging to noncrystalline titanium with coordination number of 4−6 consistent with literature reports.[43−46,75] The other two catalysts have absorption at lower wavelength of 210 nm often attributed to tetra-coordinated titanium.[76,77] The absorption bands for anatase TiO_2 at 330 nm and hexa-coordinated titanium species at ca. 270 nm were not present in Ti-MT1 and Ti-MS1. The same phenomenon was also observed in related publications on preparation of mesoporous titanosilicates using zeolite precursors.[43−46,75] Ti-MT1 and Ti-MS1 have absorption bands that are comparable to TS-1 suggesting that the coordination environment of titanium species in Ti-MT1 and Ti-MS1 is similar to TS-1. Thus, the dissimilarity between Ti-MCM-41 from Ti-MT1 and Ti-MS1 are obvious and could have implication on the catalytic properties of these materials.

The experimental results show that seeds are necessary for the incorporation of zeolitic structure in the mesoporous catalysts. The fact that the mesoporous catalysts prepared from nanocrystal seeds of very different compositions have near identical titanium content and sites (i.e., tetra- vs octa-coordinated titanium) suggests that the seeds did not simply dissolve to supply the zeolitic structure found in these samples. Indeed, the seeds appear to actively promote the formation of zeolitic structures in Ti-MT1 and Ti-MS1. One plausible means is that the seed organizes the primary and secondary building units into zeolite on its surface, which redissolve under synthesis into zeolite fragments that are then captured and incorporated into the mesopores. The process could be driven by Ostwald ripening as the disparity in the growth rates of zeolite and mesoporous material is great. This hypothesis could also explain the presence of unconsumed TS-1 seeds in Ti-MT1 and the similarity of the composition and chemistry of Ti-MT1 and Ti-MS1 catalysts despite the lack of titanium in the TPA-Sil-1 seeds.

The ordered domains of zeolite structures and fragments in the pore walls of the Ti-MS1 and Ti-MT1 are believed to be mainly responsible for their high structural stability under hydrothermal conditions (Figure 1b).[78] It is also speculated that the preponderance of tetra-coordinated titanium (i.e., 210 nm absorbance) in Ti-MS1 and Ti-MT1 are indicative of the crystalline nature of the pore wall and thus its greater stability.[43,44,46,47,79]

3.3. Hydroxylation of Aromatic Compounds. The mesoporous catalysts were investigated for benzene, phenol, and

dx.doi.org/10.1021/cm201619y |*Chem. Mater.* 2011, 23, 4469–4479

Table 2. Catalytic Activities in Benzene, Phenol, and Styrene Hydroxylation over TS-1, Ti-MCM-41, Ti-MT1, and Ti-MS1[a]

	benzene hydroxylation		phenol hydroxylation			styrene hydroxylation			
catalysts	X_{BEN} (%)	S_{PHE} (%)	X_{PHE} (%)	S_{CAT} (%)	S_{HQ} (%)	X_{STY} (%)	S_{PAC} (%)	S_{BAL} (%)	S_{SO} (%)
TS-1	3.2	95.5	20.6	50.5	46.5	20.2	80.3	17.2	1.8
Ti-MCM-41	17.9	98.1	5.2	61.3	34.6	25.5	3.6	96.4	0.0
Ti-MT1	24.7	98.5	10.6	53.1	42.2	28.6	45.3	51.1	2.6
Ti-MS1	25.5	99.2	10.9	52.2	45.1	31.3	48.6	47.1	3.1

[a] Reaction time: 6 h; X_{BEN}, X_{PHE}, X_{STY}: the conversion of benzene, phenol, and styrene; S_{PHE}: the selectivity of phenol; S_{CAT}, S_{HQ}: the selectivity of catechol and hydroquionone; S_{PAC}, S_{BAL}, S_{SO}: the selectivity of phenylacetaldehyde, benzaldehyde, and styrene epoxide.

styrene hydroxylation reactions, and the reaction conversions are plotted in Figure 7 and summarized in Table 2. A comparison was made with TS-1 zeolite (Si/Ti = 50) and MCM-41 mesoporous silica. The MCM-41 is inert and does not catalyze the reactions. TS-1 is very active for the hydroxylation of phenol as reported in the literature. It is also an active catalyst for the hydroxylation of benzene and styrene.[15−19] The styrene conversion over TS-1 is modest due to slow diffusion of the bulky molecules in the zeolite pores. The selectivities of TS-1 for benzene, phenol, and styrene hydroxylations are 96% for phenol, 97% for dihydroxybenzene (catechol and hydroquinone), and 80% for phenylacetaldehyde, respectively. TS-1 and Ti-MCM-41 have comparable catalytic activity compared to the publications.[15,43,44,80−85]

The reaction results in Figure 7 show that Ti-MS1 and Ti-MT1 are more active than Ti-MCM-41 for all three reactions and are also more active than TS-1 for benzene and styrene hydroxylation reactions. The lower reactivity of the mesoporous catalysts for phenol hydroxylation compared to TS-1 is understandable as the zeolitic structure in these catalysts (Figures 4 and 6) lacks the long-range order and connectivity of TS-1 zeolite. Ti-MS1 and Ti-MT1 have similar reactivity for benzene and phenol hydroxylation reactions, but Ti-MS1 is the better catalyst for styrene hydroxylation. All three mesoporous catalysts have better than 98% selectivity for phenol in benzene hydroxylation reaction and higher than 95% selectivity for dihydroxybenzene in phenol hydroxylation reaction. For the styrene hydroxylation reaction, the mesoporous catalysts are selective to aromatic acetaldehydes (i.e., phenylacetaldehyde and benzaldehyde) where Ti-MCM-41, Ti-MT1, and Ti-MS1 have selectivities of 100, 96.4, and 95.7%, respectively.

Overall, Ti-MS1 performs best for all three hydroxylation reactions followed by Ti-MT1 and Ti-MCM-41. The low conversion observed for Ti-MCM-41 is attributed to the nature of the titanium sites in this catalyst.[44] The poor reactivity of Ti-MCM-41 correlates well with its low content of tetrahedrally coordinated titanium atoms (i.e., Titetra/Tiocta = 1.1 versus 1.5 for Ti-MT1 and 1.5 for Ti-MS1).

The conversion and selectivities of the mesoporous Ti-MCM-41, Ti-MS1, and Ti-MT1 and microporous TS-1 catalysts are shown in Table 2. The product distribution from phenol hydroxylation reaction is comparable for Ti-MS1, Ti-MT1, and TS-1 catalyst, while Ti-MCM-41 produced more catechol. The product selectivities for phenylacetaldehyde, benzaldehyde, and styrene oxide are very different for the catalysts. TS-1 produced mainly phenylacetaldehyde, while benzaldehyde is the main product of Ti-MCM-41. Ti-MS1 and Ti-MT1 display similar product selectivities. These results are consistent with the structural and compositional variations in these catalysts. Prior works have established TS-1 to be more active for phenol hydroxylation than ordered mesoporous titanosilicates,[43,44] while benzene hydroxylation is better catalyzed by the mesoporous catalysts.[36] It had been proposed that the polarity and size of the benzene and phenol could explain the observed reaction trend over the TS-1 and mesoporous titanosilicates.[87,88]

3.4. Mesoporous Catalyst Deactivation and Regeneration. Catalyst deactivation was investigated by reusing the catalysts in three successive batch reactions with each run lasting six hours. The catalysts were recovered, washed, dried, and weighed. Benzene, phenol, and styrene conversions are plotted in Figure 8a, c, and e for Ti-MCM-41, Ti-MT1, and Ti-MS1 mesoporous catalysts. Ti-MCM-41 suffers rapid deactivation losing half its activity in benzene and phenol hydroxylation after the second reaction run and roughly 80% of its initial activity at the end of the third reaction. X-ray diffraction of the spent Ti-MCM-41 catalyst shows a disappearance of ordered mesopore indicating possible pore collapse during the reaction (Figure 9). However, the selectivity remains unchanged with deactivation. A better than 95% selectivity in phenol was obtained from benzene and about 93% selectivity in dihydroxybenzenes from phenol. Styrene hydroxylation shows that the selectivity of Ti-MCM-41 for aromatic aldehydes decreased slightly from 100% to above 90% after the third reaction run.

The Ti-MT1 and Ti-MS1 mesoporous catalysts deactivate less as shown in Figure 8a, c, and e. This could be due to incorporation of zeolitic fragments and SBU as well as having thicker pore walls. Being better equipped to withstand severe reaction conditions (Figure 1), these catalysts retained their ordered mesoporous structure following the reactions (Figure 9). Ti-MT1 suffered a 40% drop in conversion for benzene hydroxylation after the third reaction run and a 55% decrease for phenol hydroxylation. Ti-MS1 performed better displaying respectively a 35% and a 40% decrease in conversion for the hydroxylation of benzene and phenol. Both mesoporous catalysts have high selectivity (i.e., > 97% for phenol and >92% for dihydroxybenzene). Ti-MT1 catalyst activity decreased 25% after third styrene hydroxylation reaction with a concomitant drop in selectivity for aromatic aldehydes from 96% to slightly higher than 88%. Ti-MS1 suffered similar drop in conversion but maintained selectivity higher than 87%.

Catalyst regeneration by air calcinations was examined in a separate study, and the results are plotted in Figure 8b, d, and f. It is clear from the plots that Ti-MCM-41 still suffered from considerable deactivation in each reaction run. This is strong evidence that

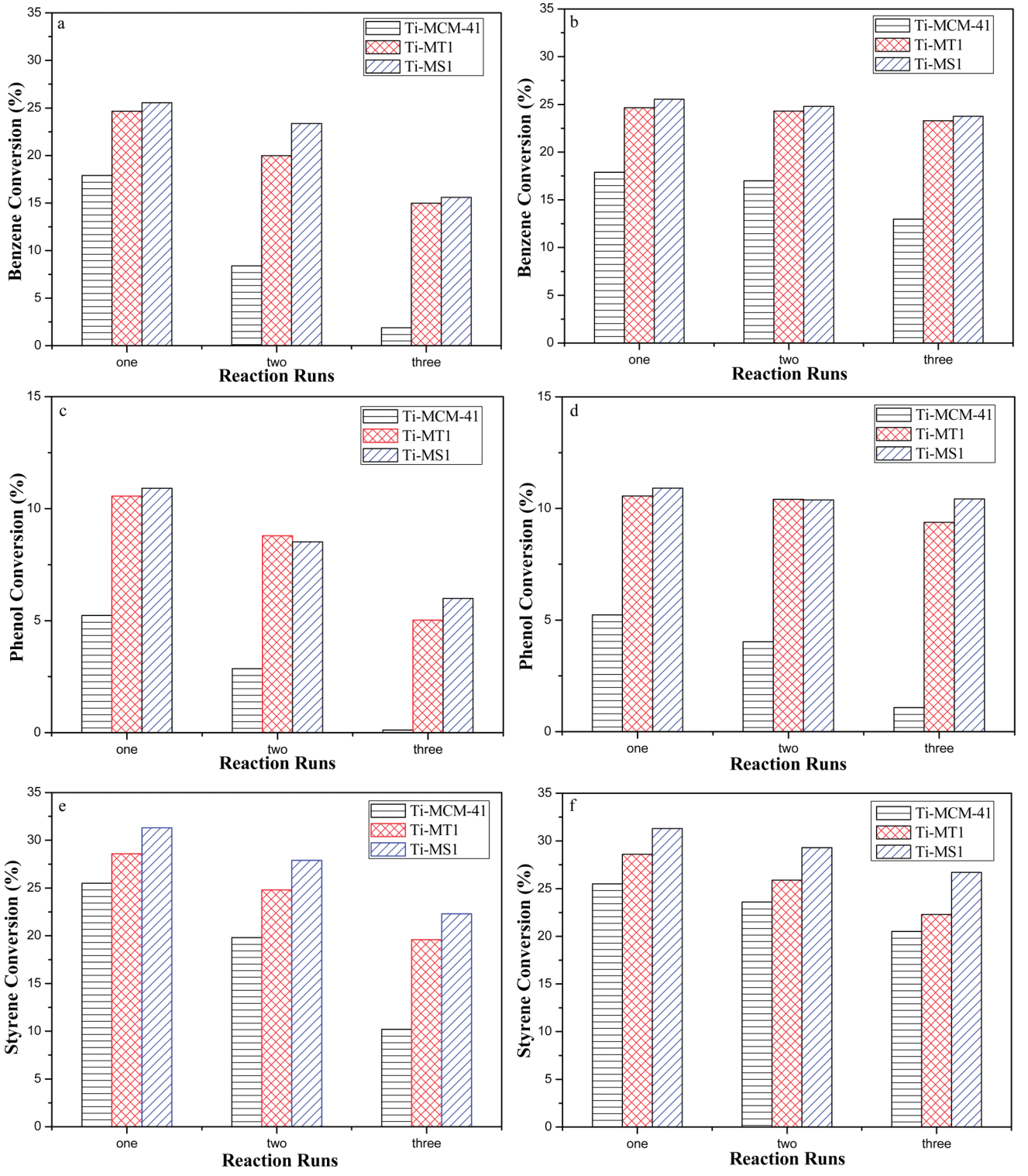

Figure 8. Plots of benzene (a, b), phenol (c, d), and styrene conversions (e, f) after each reactions with (b, d, f) and without calcinations (a, c, e).

the deactivation observed in Ti-MCM-41 results from the lost of mesoporous structure. Ti-MT1 and Ti-MS1 maintain their conversion in benzene and phenol hydroxylation reactions with the selectivity of 99% for phenol and 95% for dihydroxybenzene, respectively. This suggests that the deactivation of these catalysts is mainly from strongly adsorbed organic molecules and possible carbon deposition. Figure 8f shows that catalyst deactivation during styrene hydroxylation reaction cannot be completely recovered by air calcinations. All three catalysts suffer similar extent of deactivation. The lost of selectivity for aromatic aldehydes indicates a possible lost of tetrahedrally coordinated titanium during reaction.

dx.doi.org/10.1021/cm201619y |*Chem. Mater.* 2011, 23, 4469–4479

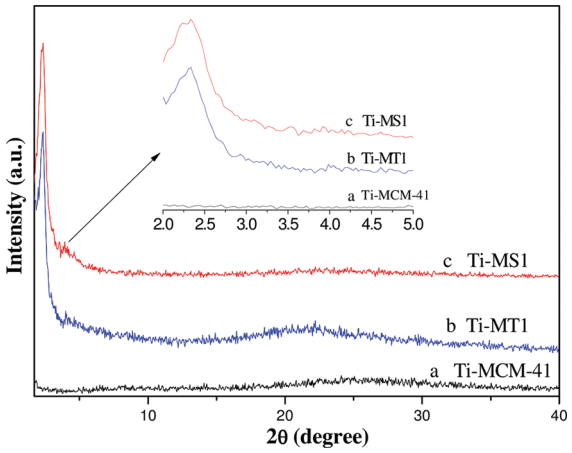

Figure 9. X-ray diffraction patterns of (a) Ti-MCM-41, (b) Ti-MT1, and (c) Ti-MS1 after reaction study.

4. CONCLUDING REMARKS

This work shows that titania-silica mesoporous catalyst (Ti-MCM-41) prepared by conventional methods was not only less active but also unstable in hydroxylation reactions. Catalyst deactivation was rapid and caused by lost of mesopore structure. This poor structural stability was also observed during a hydrothermal test. Ti-MT1 and Ti-MS1 prepared with the addition of TPA-TS-1 and TPA-Sil-1 nanocrystal seeds are active and stable catalysts. Both catalysts survive with intact mesopores in hydrothermal tests and reaction study. TOF-SIMS and FTIR techniques detected 5−1 SBU fragments and zeolitic structures in these two catalysts. Most of the titanium in these catalysts was tetrahedrally coordinated compared to mostly octahedral titanium sites found in Ti-MCM-41. Ti-MT1 had a composite structure consisting of coexisting TS-1 zeolite and mesopore domains as indicated by XRD results. This could be responsible for the greater disorder observed in this catalyst and poorer stability when compared to Ti-MS1. The similarity in reactivity of Ti-MT1 and Ti-MS1 prepared from TS-1 and Sil-1 nanocrystal seeds dispels the idea that the nanocrystal seeds function merely as a source of the zeolite fragments incorporated in the pore walls but instead suggest that the nanocrystal seeds either work to stabilize or promote the incorporation of SBU from the solution. In contrast to Ti-MCM-41, Ti-MS1 with thermally stable active sites could be prepared by assembling from Sil-1 nanoparticles, and the appearance of a mixture phase (Ti-MT1) is avoided.

AUTHOR INFORMATION

Corresponding Author

*Phone: +86 411 84986155. Fax: +86 411 84986155. E-mail: xfzhang@dlut.edu.cn (X.F.Z.). Phone: +86 411 84986080. Fax: +86 411 84986080. E-mail: jqiu@dlut.edu.cn (J.S.Q.). Phone: +852 2358 7123. Fax: +852 2358 0054. E-mail: kekyeung@ust.hk (K.L.Y.).

ACKNOWLEDGMENT

This work was partly supported by the National Natural Science Foundation of China (Grant No. 20673017, 21036006, 21173030), PetroChina Innovation Foundation (Grant No. 2008D-5006-05-06), Program for Liaoning Excellent Talents in University (Grant No. LR201008), and Universities Science & Research Project of Liaoning Province Education Department (Grant No. 2009S019). The authors also thank the Materials Characterization and Preparation Facility (MCPF) and the Advanced Engineering Material Facility (AEMF) of the Hong Kong University of Science and Technology for the samples characterizations.

REFERENCES

(1) Taramasso, M.; Perego, G.; Notari, B. U.S. Patent 4410501, 1983.
(2) Wan, Y. S. S.; Chau, J. L. H.; Gavriilidis, A.; Yeung, K. L. *Chem. Commun.* **2002**, *8*, 878.
(3) Wan, Y. S. S.; Chau, J. L. H.; Yeung, K. L.; Gavriilidis, A. *J. Catal.* **2004**, *223*, 241.
(4) Wan, Y. S. S.; Yeung, K. L.; Gavriilidis, A. *Appl. Catal., A* **2005**, *281*, 285.
(5) Cao, S. L.; Yeung, K. L.; Yue, P. L. *Appl. Catal., B* **2007**, *76*, 64.
(6) Cao, S. L.; Yeung, K. L.; Kwan, J. K. C.; To, P. M. T.; Yu, S. C. T. *Appl. Catal., B* **2009**, *86*, 127.
(7) Ho, K. Y.; Yeung, K. L. *J. Catal.* **2006**, *242*, 131.
(8) Ho, K. Y.; Yeung, K. L. *Gold Bull.* **2007**, *40*, 15.
(9) Yeung, K. L; Maira, A. J.; Stolz, J.; Hung, E. W. C.; Ho, N. K. C.; Wei, A. C.; Soria, J.; Chao, K. J.; Yue, P. L. *J. Phys. Chem. B* **2002**, *106*, 4608.
(10) Maira, A. J.; Lau, W. N.; Lee, C. Y.; Yue, P. L.; Chan, C. K.; Yeung, K. L. *Chem. Eng. Sci.* **2003**, *58*, 959.
(11) Atienzar, P.; Valencia, S.; Corma, A.; Garcia, H. *Chem. Phys. Chem.* **2007**, *8*, 1115.
(12) Coakley, K. M.; McGehee, M. D. *Appl. Phys. Lett.* **2003**, *83*, 3380.
(13) Dusi, M. T.; Mallat, T.; Baiker, A. *Catal. Rev. - Sci. Eng.* **2000**, *42*, 213.
(14) Corma, A.; Garcia, H. *Chem. Rev.* **2002**, *102*, 3837.
(15) Laha, S. C.; Kumar, R. *J. Catal.* **2001**, *204*, 64.
(16) Bianchi, D.; D'Aloisio, R.; Bortolo, R.; Ricci, M. *Appl. Catal., A* **2007**, *327*, 295.
(17) Wang, X. B.; Zhang, X. F.; Liu, H. O.; Yeung, K. L.; Wang, J. Q. *Chem. Eng. J.* **2010**, *156*, 562.
(18) Wang, X. B.; Guo, Y.; Zhang, X. F.; Wang, Y.; Liu, H. O.; Wang, J. Q.; Qiu, J. S.; Yeung, K. L. *Catal. Today* **2010**, *156*, 288.
(19) Wang, X. B.; Zhang, X. F.; Wang, Y.; Liu, H. O.; Qiu, J. S.; Wang, J. Q.; Han, W.; Yeung, K. L. *ACS Catal.* **2011**, *1*, 437.
(20) Xin, H. C.; Zhao, J.; Xu, S. T.; Li, J. P.; Zhang, W. P.; Guo, X. W.; Hensen, E. J. M.; Yang, Q. H.; Li, C. *J. Phys. Chem. C* **2010**, *114*, 6553.
(21) Kresge, C. T.; Leonowicz, M. E.; Roth, W. J.; Vartuli, J. C.; Beck, J. S. *Nature* **1992**, *359*, 710.
(22) Bagshaw, S. A.; Prouzet, E.; Pinnavaia, T. J. *Science* **1995**, *269*, 1242.
(23) Zhao, D. Y.; Huo, Q. S.; Feng, J. L.; Chmelka, B. F.; Stuck, G. D. *J. Am. Chem. Soc.* **1998**, *120*, 6024.
(24) Schuth, F. *Stud. Surf. Sci. Catal.* **2004**, *148*, 1.
(25) Taguchi, A.; Schuth, F. *Microporous Mesoporous Mater.* **2005**, *77*, 1.
(26) De Vos, D. E.; Dams, M.; Sels, B. F.; Jacobs, P. A. *Chem. Rev.* **2002**, *102*, 3615.
(27) Anpo, M.; Takeuchi, M. *J. Catal.* **2003**, *216*, 505.
(28) Lam, K. F.; Yeung, K. L.; McKay, G. *Langmuir* **2006**, *22*, 9632.
(29) Lam, K. F.; Yeung, K. L.; McKay, G. *J. Phys. Chem. B* **2006**, *110*, 2187.
(30) Lam, K. F.; Yeung, K. L.; McKay, G. *Environ. Sci. Technol.* **2007**, *41*, 3329.
(31) Lam, K. F.; Yeung, K. L.; McKay, G. *Microporous Mesoporous Mater.* **2007**, *100*, 191.
(32) Lam, K. F.; Fong, C. M.; Yeung, K. L. *Gold Bull.* **2007**, *40*, 192.
(33) Pasqua, L.; Cundari, S.; Ceresa, C.; Cavaletti, G. *Curr. Med. Chem.* **2009**, *16*, 3054.
(34) Vallet-Regi, M.; Balas, F.; Arcos, D. *Angew. Chem., Int. Ed.* **2007**, *46*, 7548.
(35) Corma, A.; Navarro, M. T.; Pariente, J. P. *J. Chem. Soc., Chem. Commun.* **1994**, 147.

(36) Tanev, P. T.; Chibwe, M.; Pinnavaia, T. J. *Nature* **1994**, *368*, 321.
(37) Schmidt, I.; Krogh, A.; Wienberg, K.; Carlsson, A.; Brorson, M.; Jacobsen, C. J. H. *Chem. Commun.* **2000**, 2157.
(38) Zhang, W. Z.; Pauly, T. R.; Pinnavaia, T. J. *Chem. Mater.* **1997**, *9*, 2491.
(39) Wu, P.; Tatsumi, T.; Komatsu, T.; Yashima, T. *Chem. Mater.* **2002**, *14*, 1657.
(40) Karlsson, A.; Stöcker, M.; Schmidt, R. *Microporous Mesoporous Mater.* **1999**, *27*, 181.
(41) Trong, On, D.; Lutic, D.; Kaliaguine, S. *Microporous Mesoporous Mater.* **2001**, *44*−*45*, 435.
(42) Zhang, Z. T.; Han, Y.; Zhu, L.; Wang, R. W.; Yu, Y.; Qiu, S. L.; Zhao, D. Y.; Xiao, F. S. *Angew. Chem., Int. Ed.* **2001**, *40*, 1258.
(43) Xiao, F. S.; Han, Y.; Yu, Y.; Meng, X.; Yang, M.; Wu, S. *J. Am. Chem. Soc.* **2002**, *124*, 888.
(44) Meng, X. J.; Li, D. F.; Yang, X. Y.; Yu, Y.; Wu, S.; Han, Y.; Yang, Q.; Jiang, D. Z.; Xiao, X. S. *J. Phys. Chem. B* **2003**, *107*, 8972.
(45) Yang, X. Y.; Han, Y.; Lin, K. F.; Tian, G.; Feng, Y. F.; Meng, X. J.; Di, Y.; Du, Y. C.; Zhang, Y. L.; Xiao, F. S. *Chem. Commun.* **2004**, 2612.
(46) Han, Y.; Wu, S.; Sun, Y. Y.; Li, D. S.; Xiao, F. S.; Liu, J.; Zhang, X. *Chem. Mater.* **2002**, *14*, 1144.
(47) MacLachlan, M. J.; Coombs, N.; Ozin, G. A. *Nature* **1999**, *397*, 681.
(48) Liu, Y.; Zhang, W. Z.; Pinnavaia, T. J. *J. Am. Chem. Soc.* **2000**, *122*, 8791.
(49) Tanaka, S.; Nakatani, N.; Okada, H.; Miyake, Y. *Top. Catal.* **2010**, *53*, 224.
(50) Reichinger, M.; Gies, H.; van den Berg, M.; Gruenert, W.; Kirschhock, C. *Stud. Surf. Sci. Catal.* **2007**, *170*, 276.
(51) Li, P.; Liu, L. P.; Xiong, G. *Phys. Chem. Chem. Phys.* **2011**, *13*, 11248.
(52) Čejka, J.; Mintova, S. *Catal. Rev. - Sci. Eng.* **2007**, *49*, 457.
(53) Prokešová-Fojtíková, P.; Mintova, S.; Čejka, J.; Žilková, N.; Zukal, A. *Microporous Mesoporous Mater.* **2006**, *92*, 154.
(54) Prokešová, P.; Mintova, S.; Čejka, J.; Bein, T. *Mater. Sci. Eng., C* **2003**, *23*, 1001.
(55) Prokešová, P.; Mintova, S.; Čejka, J.; Bein, T. *Microporous Mesoporous Mater.* **2003**, *64*, 165.
(56) Petkov, N.; Hölzl, M.; Metzger, T. H.; Mintova, S.; Bein, T. *J. Phys. Chem. B* **2005**, *109*, 4485.
(57) Qiu, F. R.; Wang, X. B.; Zhang, X. F.; Liu, H. O.; Liu, S. Q.; Yeung, K. L. *Chem. Eng. J.* **2009**, *147*, 316.
(58) Naik, S. P.; Chiang, A. S. T.; Thompson, R. W.; Huang, F. C.; Kao, H. M. *Microporous Mesoporous Mater.* **2003**, *60*, 213.
(59) Naik, S. P.; Chiang, A. S. T.; Thompson, R. W. *J. Phys. Chem. B* **2003**, *107*, 7006.
(60) Naik, S. P.; Chiang, A. S. T.; Thompson, R. W.; Huang, F. C. *Chem. Mater.* **2003**, *15*, 787.
(61) Naik, S. P.; Chiang, A. S. T.; Sasakura, H.; Yamaguchi, Y.; Okubo, T. *Chem. Lett.* **2005**, *34*, 982.
(62) Igarashi, N.; Hashimoto, K.; Tatsumi, T. *Microporous Mesoporous Mater.* **2007**, *104*, 269.
(63) Au, L. T. Y.; Mui, W. Y.; Lau, P. S.; Ariso, C. T.; Yeung., K. L. *Microporous Mesoporous Mater.* **2001**, *47*, 203.
(64) Thangaraj, A.; Sivasanker, S. *J. Chem. Soc., Chem. Commun.* **1992**, 124.
(65) Thangaraj, A.; Eapan, M. J.; Sivasanker, S.; Ratnasamy, R. *Zeolites* **1992**, *12*, 943.
(66) Kruk, M.; Jaroniec, M.; Sayari, A. *Chem. Mater.* **1999**, *11*, 492.
(67) Zhou, Z. H.; Lu, J. M.; Wu, S. F.; Zhou, J. L.; Wang, J. Q. *J. Inorg. Mater.* **2009**, *24*, 325.
(68) Han, W.; Yeung, K. L.; Weng L. T. (unpublished data).
(69) Reddy, J. S.; Sayari, A. *Stud. Surf. Sci. Catal.* **1995**, *94*, 309.
(70) Davis, R. J.; Liu, Z. *Chem. Mater.* **1997**, *9*, 2311.
(71) Mukhopahyay, S. M.; Garofalini, S. H. *J. Non-Cryst. Solids* **1990**, *126*, 202.
(72) Stakheev, A. Y.; Shpiro, E. S.; Apijok, J. *J. Phys. Chem.* **1993**, *97*, 5668.
(73) Deo, G.; Turek, A. M.; Wachs, I. E.; Huybrechts, D. R. C.; Jacobs, P. A. *Zeolites* **1993**, *13*, 365.
(74) Trong ON, D.; Bonneviot, L.; Bittar, A.; Sayari, A.; Kaliaguine, S. *J. Mol. Catal.* **1992**, *74*, 233.
(75) Jin, C. Z.; Li, G.; Wang, X. S.; Zhao, L. X.; Liu, L. P.; Liu, H. O. *Chem. Mater.* **2007**, *19*, 1664.
(76) Klein, S.; Weckhuysen, B. M.; Martens, J. A.; Maier, W. F.; Jacobs, P. A. *J. Catal.* **1996**, *163*, 489.
(77) Petrini, G.; Cesana, A.; De Alberti, G.; Genoni, F.; Leofanti, G.; Padovan, M.; Paparatto, G.; Rofia, P. *Stud. Surf. Sci. Catal.* **1991**, *68*, 761.
(78) Corma, A. *Chem. Rev.* **1997**, *97*, 2373.
(79) Han, Y.; Xiao, F. S.; Wu, S.; Sun, Y.; Meng, X.; Li, D.; Lin, S.; Deng, F.; Ai, X. *J. Phys. Chem. B* **2001**, *105*, 7963.
(80) Zhuang, J. Q.; Ma, D.; Yan, Z. M.; Liu, X. M.; Han, X. W.; Bao, X. H.; Zhang, Y. H.; Guo, X. W.; Wang, X. S. *Appl. Catal., A* **2004**, *258*, 1–6.
(81) Gao, H. X.; Lu, W. K.; Chen, Q. L. *Microporous Mesoporous Mater.* **2000**, *34*, 307.
(82) Yube, K.; Furuta, M.; Mae, K. *Catal. Today* **2007**, *125*, 56.
(83) Ke, X. B.; Xu, L.; Zeng, C. F.; Zhang, L. X.; Xu, N. P. *Microporous Mesoporous Mater.* **2007**, *106*, 68.
(84) Lin, K. F.; Sun, Z. H.; Lin, S.; Jiang, D. Z.; Xiao, F. S. *Microporous Mesoporous Mater.* **2004**, *72*, 193.
(85) Wang, G. J.; Liu, G. Q.; Xu, M. X.; Yang, Z. X.; Liu, Z. W.; Liu, Y. W.; Chen, S. F.; Wang, L. *Appl. Surf. Sci.* **2008**, *255*, 2632.
(86) Bengoa, J. F.; Gallegos, N. G.; Marchetti, S. G.; Alvarez, A. M.; Cagnoli, M. V.; Yeramián, A. A. *Microporous Mesoporous Mater.* **1998**, *24*, 163.
(87) He, J.; Xu, W. P.; Evans, D. G.; Duan, X.; Li, C. Y. *Microporous Mesoporous Mater.* **2001**, *44*−*45*, 581.
(88) Langhendries, G.; De Vos, D. E.; Baron, G. V.; Jacobs, P. A. *J. Catal.* **1999**, *187*, 453.